# Important Role of Endothelial Caveolin-1 in the Protective Role of Endothelium-dependent Hyperpolarization Against Nitric Oxide–Mediated Nitrative Stress in Microcirculation in Mice

*Hiroki Saito, MD, PhD,* Shigeo Godo, MD, PhD,* Saori Sato, BSc,* Akiyo Ito, MD,* Yosuke Ikumi, MD,* Shuhei Tanaka, MD,* Tomoaki Ida, PhD,† Shigemoto Fujii, PhD,† Takaaki Akaike, MD, PhD,† and Hiroaki Shimokawa, MD, PhD**

**Aims:** Nitric oxide (NO) and endothelium-dependent hyperpolarization (EDH) play important roles in maintaining cardiovascular homeostasis. We have previously demonstrated that endothelial NO synthase (eNOS) plays diverse roles depending on vessel size, as a NO generating system in conduit arteries and an EDH-mediated system in resistance arteries, for which caveolin-1 (Cav-1) is involved. However, the physiological role of endothelial Cav-1 in microvessels remains to be elucidated.

**Methods and Results:** We newly generated endothelium-specific Cav-1-knockout (eCav-1-KO) mice. eCav-1-KO mice showed loss of endothelial Cav-1/eNOS complex and had cardiac hypertrophy despite normal blood pressure. In eCav-1-KO mice, as compared to wild-type controls, the extent of eNOS phosphorylation at inhibitory Thr495 was significantly reduced in mesenteric arteries and the heart. Isometric tension and Langendorff-perfused heart experiments showed that NO-mediated responses were enhanced, whereas EDH-mediated responses were reduced in coronary microcirculation in eCav-1-KO mice. Immunohistochemistry showed increased level of 8-nitroguanosine 3′,5′-cyclic monophosphate (8-nitro-cGMP), a marker of nitrative stress, in the heart from eCav-1-KO mice. S-guanylation of cardiac H-Ras in eCav-1-KO mice was also significantly increased compared with wild-type controls.

**Conclusions:** These results suggest that eCav-1 is involved in the protective role of EDH against nitrative stress caused by excessive NO to maintain cardiac microvascular homeostasis.

**Key Words:** endothelium-dependent hyperpolarization, nitric oxide, nitric oxide synthase, caveolin-1

(*J Cardiovasc Pharmacol*™ 2018;71:113–126)

## INTRODUCTION

The endothelium plays important roles in modulating vascular tone by synthesizing and releasing several vasodilator substances, collectively named as endothelium-derived relaxing factors (EDRFs), including vasodilator prostaglandins [mainly prostacyclin ($PGI_2$)], nitric oxide (NO), and endothelium-dependent hyperpolarization (EDH) factors.[1–3] The most characterized EDRF is NO. Accumulating evidence has demonstrated that NO plays crucial roles not only in vascular relaxation but also in many beneficial cardiovascular functions.[1–3] EDH factors were independently discovered by Feletou and Vanhoutte[4] and Chen et al[5] as a factor released by the endothelium that causes hyperpolarization and relaxation of underlying vascular smooth muscle cells (VSMCs). It is widely accepted that the contribution of EDRFs to endothelium-dependent vasodilatation varies depending on vessel size; NO predominantly regulates the tone of large conduit vessels and the contribution of NO decreases as vessel size decreases, whereas that of EDH increases as vessel size decreases.[1,6,7] Although the nature of EDH has not been fully elucidated, several candidates have been proposed to serve as EDH factors in different species and vascular beds.[1–3] We have previously demonstrated that endothelium-derived hydrogen peroxide ($H_2O_2$) is an EDH factor in mouse[8] and human mesenteric arteries[9] and porcine coronary microvessels.[10] We also have demonstrated that endothelial NO synthase (eNOS) is a major source of the EDH factor, where Cu,Zn-superoxide dismutase (Cu, Zn-SOD) catalyzes eNOS-derived superoxide anions to $H_2O_2$.[11,12] Thus, eNOS plays diverse roles depending on vessel size, as a NO-generating system in conduit arteries and an EDH-mediated system in resistance arteries.[1] Recently, we also have demonstrated that endothelial caveolin-1 (Cav-1) is involved in the mechanisms for the enhanced EDH-mediated responses in resistance arteries in mice.[13,14]

Received for publication April 10, 2017; accepted October 2, 2017.

From the Departments of *Cardiovascular Medicine; and †Environmental Health Sciences and Molecular Toxicology, Tohoku University Graduate School of Medicine, Sendai, Japan.

Supported in part by a Grant-in-Aid for Scientific Research on Innovative Areas (Signaling Functions of Reactive Oxygen Species), a Grant-in-Aid for Tohoku University Global COE for Conquest of Signal Transduction Diseases with Network Medicine, and the Grant-in-Aid for Scientific Research (16K19383), all of which are from the Ministry of Education, Culture, Sports, Science, and Technology, Tokyo, Japan.

The authors report no conflicts of interest.

Reprints: Hiroaki Shimokawa, MD, PhD, Department of Cardiovascular Medicine, Tohoku University Graduate School of Medicine, 1-1 Seiryo-machi, Aoba-ku, Sendai 980-8574, Japan (e-mail: shimo@cardio.med.tohoku.ac.jp).

Among the 3 isoforms of caveolin (Cav-1–3), Cav-1 and Cav-2 are abundant in endothelial cells, adipocytes, and fibroblasts,[15] whereas Cav-3 is mainly expressed in cardiac, skeletal, and smooth muscle cells.[16] It is known that Cav-1 expression is required to stabilize Cav-2 protein.[17] Cav-1 is a main protein component of the caveolae, flask-shaped invaginations of the plasma membrane and is essential for caveolae formation.[18] In the caveolae, Cav-1 interacts with several intracellular signaling molecules, such as G protein-coupled receptors, tyrosine kinases, GTPases, and eNOS.[19] Importantly, Cav-1 suppresses the function of eNOS by binding with its scaffolding domain, resulting in the inhibition of NO release from eNOS.[19] It has been reported that systemic Cav-1-KO mice show cardiac hypertrophy, in which altered eNOS function is involved.[14] Although the relationship between endothelial Cav-1 (eCav-1) and cardiac hypertrophy has been postulated, the broad distribution of Cav-1 has made it difficult to understand the precise roles of eCav-1 and the pathogenesis of cardiac hypertrophy in systemic Cav-1-KO mice. In this study, we thus aimed to elucidate the role of endothelial Cav-1 in cardiac homeostasis, with a special reference to cardiac hypertrophy, in newly generated endothelium-specific caveolin-1-knockout (eCav-1-KO) mice.

## MATERIALS AND METHODS

### Animals

This study was reviewed and approved by the Committee on Ethics of Animal Experiments of Tohoku University (2013MdA-477), which was granted by the Guide for Care and Use of Laboratory Animals published by the US National Institutes of Health. Male mice aged 10–16 weeks were used in this study. We newly generated Cav-1-floxed (Cav-1flox/flox) mice, in which Cav-1 exon 3 is flanked by 2 loxP sites on the C57BL6 background (Unitech Co, Kashiwa, Japan). To generate eCav-1-KO mice, Cav-$1^{flox/flox}$ mice were cross-bred with Tie2-Cre mice (Jackson Laboratory, Bar Harbor, ME). Cav-$1^{flox/flox}$ Tie2-Cre positive mice were used as eCav-1-KO mice and Cav-$1^{flox/flox}$ Tie2-Cre negative mice as wild-type (WT) control in this study. The genotype of the mice was confirmed by polymerase chain reaction using primers specific for the targeted gene (5′-TATTCTCCTTGCTCTAATGTCACCT-3′ and 5′-ACAGTGAGGGTCTTTGAAGATGTTA-3′) and the Tie2-Cre transgene (5′-GCGGTCTGGCAGTAAAAACTATC-3′ and 5′-GTGAAACAGCATTGCTGTCACTT-3′). They were maintained in the Laboratory of Animal Experiments in Tohoku University. All animals were maintained in accordance with the rules and regulations configured by the committee, fed standard rodent chow, and maintained on 12-hour light/dark cycles.

### Immunohistochemistry

After perfusion fixation with 4% paraformaldehyde, whole mesenteries and whole hearts were harvested, immersed in 4% paraformaldehyde overnight, and washed in 10%, 20%, and 30% sucrose containing phosphate-buffered saline for 6 hours each at 4°C.[20] Then, they were embedded in optimal cutting temperature compound (Sakura, Tokyo, Japan), and cut into 10 μm-thick slices. Each slice were incubated with first antibodies overnight at 4°C, followed by incubation with each secondary antibodies for 1 hour at room temperature on slide glasses. Slides were observed with LSM 780 confocal microscopy (Carl Zeiss, Oberkochen, Germany) in the Zen software (Carl Zeiss).

### Western Blot Analysis

The extracted protein was separated by sodium dodecyl sulfate (SDS)-polyacrylamide gel electrophoresis and transferred to polyvinylidene difluoride membranes.

Human umbilical vein endothelial cells (Takara Bio, Inc, Otsu, Japan) and neonatal rat cardiomyocyte were used as positive control. We used human umbilical vein endothelial cell at passage 4–7 in this study. Isolation of neonatal rat cardiomyocyte was performed as previously described.[21] After incubating with HRP-conjugated anti-mouse (Sigma-Aldrich, St. Louis, MO) or anti-rabbit IgG antibody (Cell Signaling, Danvers, MA), the regions containing proteins were visualized using ECL prime western blotting detection system (Amersham Biosciences, Buckinghamshire, United Kingdom). Densitometric analysis was performed by Image J (National Institutes of Health) Software.

### Electron Microscopy

Under anesthesia, perfusion fixation was performed through the left ventricle. Tissues were perfused with fixative containing 2% paraformaldehyde and 2.5% glutaraldehyde in 0.1 mol/L cacodylate buffer. After several buffer washes, whole mesenteries and whole hearts were dissected and placed in buffer overnight. Tissues were then post-fixed in 1% osmium tetroxide for 90 minutes on ice. After several distilled water washes, tissues were en bloc stained with 1% uranyl acetate, followed by dehydration in an increasing ethanol series. After the infiltration of propylene oxide, tissues were embedded in epoxy resin. Sections were stained with 2% uranyl acetate, 1% lead acetate, 1% lead nitrate, and 1% lead citrate. Sections were observed with the Hitachi transmission electron microscope H-7600 (Hitachi, Tokyo, Japan).

### Echocardiography

We performed transthoracic echocardiography with Vevo 2100 Imaging System (VisualSonics, Toronto, Canada). Mice were anesthetized with 0.5%–0.8% isoflurane to keep heart rate at approximately 500 bpm on a warm stage. Left ventricular end-diastolic diameter, left ventricular end-systolic diameter, intraventricular septal thickness, posterior wall thickness, fractional shortening, and ejection fraction were measured in M-mode images at the papillary muscle level. All measurements were averaged from 3 to 5 beats.

### Telemetry Experiments

Telemetry experiments were performed as described previously.[20] The mice were anesthetized with 1.5%–2% isoflurane in 190–200 mL of room air per minute during the operation. A telemetry probe catheter was inserted into the aortic arch through the left carotid artery. The telemetry transmitter unit (TA11PA-C10; Data Sciences International,

St. Paul, MN) was then implanted under the skin. After the operation, they were housed individually on top of the telemetry receivers to allow for environmental adaptation at least for 1 week before recordings. Blood pressure and heart rate were continuously recorded on a computer-based data acquisition system (NOTOCORD HEM 4.2.0; Notocord, Paris, France).

## Immunoprecipitation

Tissues were isolated and lysed in tissue protein extraction reagent (T-PER; Thermo Fisher, Rockford, MA), followed by centrifugation. The supernatants were incubated with anti-eNOS antibody or anti-H-Ras antibody at a dilution of 1:100 for 1 hour at 4°C. As negative controls, the same amount of normal mouse IgG or rabbit IgG was used. After the incubation, 25 μL of prewashed EZ view protein G affinity gel (Sigma-Aldrich, St. Louis, MO) was added to the lysates, followed by 1-hour incubation at 4°C. After centrifugation, the supernatants were removed. After 3 times wash with T-PER, 50 μL of sample buffer (10% sodium dodecyl sulfate, 30% 2-mercaptoethanol, 20% glycerol, and 0.1% bromophenol blue) was added and heated at 95°C for 5 minutes, followed by centrifugation. The supernatants were analyzed by SDS/polyacrylamide gel electrophoresis and immunoblotting.

## Isometric Tension Experiments

We measured isometric tensions of the aorta and mesenteric arteries as previously described.[8,11,13,14,20] The mice were euthanized by intraperitoneal pentobarbital (50 mg/kg) anesthesia. The aorta and the first branches of mesenteric arteries (200–250 μm in diameter) were isolated and immersed in ice-cold Krebs–Henseleit buffer (KHB) bubbled with 95% $O_2$ and 5% $CO_2$. The aorta and small mesenteric arteries were cut into 1.0-mm rings and mounted in an organ chamber of isometric myograph (620M; Danish Myo Technology, Aarhus, Denmark). Then, the rings were stretched to the optimal resting tensions. After a 60-minute equilibration period, the rings were precontracted with phenylephrine ($10^{-6}$ mol/L). The contributions of vasodilator prostaglandins, NO, and EDH to ACh-induced endothelium-dependent relaxations were determined by the inhibitory effect of indomethacin ($10^{-5}$ mol/L), $N^{\omega}$-nitro-L-arginine (L-NNA, $10^{-4}$ mol/L), and a combination of charybdotoxin ($10^{-7}$ mol/L) and apamin ($10^{-6}$ mol/L), respectively. All the inhibitors were applied to organ chambers 30 minutes before precontraction with phenylephrine ($10^{-6}$ mol/L), except catalase (1250 units/mL) for 2 hours. To assess endothelium-independent relaxations, an NO donor sodium nitroprusside (SNP, $10^{-10}$ to $10^{-5}$ mol/L) and potassium channel opener NS-1619 ($10^{-8}$ to $10^{-4}$ mol/L) were used. Vascular responses to exogenous hydrogen peroxide ($H_2O_2$, $10^{-8}$ to $10^{-3}$ mol/L) were examined in the presence of indomethacin ($10^{-5}$ mol/L) and L-NNA ($10^{-4}$ mol/L). To remove the endothelium, luminal surface of vessels was gently rubbed with wet cotton strings.

To measure basal NO release, rings were precontracted with a submaximal dose of phenylephrine ($10^{-7}$ mol/L), and L-NNA ($10^{-4}$ mol/L) was injected at the plateau of the phenylephrine-induced contraction.[14] The responses were monitored by a computer-based analysis system using LabChart 7.0 software.

## Electrophysiological Experiments

Membrane potentials of mesenteric arteries were recorded as previously described.[13,14,20] The rings of mesenteric arteries were placed in an organ chamber perfused with 37°C KHB containing indomethacin ($10^{-5}$ mol/L) and L-NNA ($10^{-4}$ mol/L), which was bubbled with 95% $O_2$ and 5% $CO_2$. A fine glass capillary microelectrode was impaled into the vascular smooth muscle from the adventitial side. Membrane potentials were continuously monitored by a computer-based analysis system using LabChart 7.0 software.

## Langendorff-Perfused Heart Experiments

Langendorff experiments were performed as previously described.[14,20] After 10-minute heparinization (500 units intraperitoneally), the mice were anesthetized with 50 mg/kg pentobarbital sodium intraperitoneally. The hearts were isolated from the mice and then quickly placed in ice-cold KHB including 0.5 mmol/L EDTA. After all fat tissue around the aorta was removed, the aorta was carefully tied to an aortic cannula with a 21-gauge blunted needle. The heart was then perfused retrogradely 2.0 mL/min constant flow with warm KHB through the use of a Langendorff apparatus (Model IPH-W2; Primetech Corporation, Tokyo, Japan). After a 10-minute stabilization period, the heart was paced at 400 pulses/min and perfused at a constant pressure of 80 mm Hg. Coronary flow changes to agonists were measured with a flowmeter (FLSC-01; Primetech Corporation, Tokyo, Japan) and monitored by a computer-based analysis system using LabChart 7.0 software. All coronary flow values were normalized to heart weight.

## Quantitative Analysis of cGMP

Intracellular levels of cGMP were measured by liquid chromatography-tandem mass spectrometry. The hearts were isolated from the mice and homogenized in methanol with 2% acetic acid, followed by centrifugation. cGMP was extracted and purified from the supernatants by means of a preparative reverse-phase column and eluted with methanol with 15% ammonium hydroxide. The samples were then evaporated to dryness in a SpeedVac concentrator and dissolved in 0.1% formic acid, followed by centrifugation. The supernatants were analyzed using liquid chromatography-tandem mass spectrometry to detect cGMP. The debris was eluted in phosphate-buffered saline containing 10% SDS and its protein concentration was measured for normalization.

## S-Guanylation of Cardiac H-Ras Induced by Exogenous 8-nitro-cGMP

The hearts were isolated from mice and homogenized in T-PER containing 10 mmol/L β-mercaptoethanol, followed by centrifugation. The supernatants were incubated with exogenously administered 8-nitro-cGMP for 1 hour at 37°C. Then, immunoprecipitation using anti-H-Ras antibody was performed as mentioned above.

## Quantitative Analysis of 3-Nitrotyrosine

The hearts were isolated from the mice and homogenized in T-PER, followed by centrifugation. The concentrations of 3-nitrotyrosine in the heart were measured with an enzyme-linked immunosorbent assay kit (Abcam, Cambridge, MA), according to the manufacturer's instructions.

## Real-Time Polymerase Chain Reaction

Total RNA was extracted from the heart with the RNeasy universal mini kit (Quiagen, Valencia, CA). We composed complementary DNA using PrimeScript (Takara Bio Inc, Shiga, Japan) from RNA promptly according to the manufacturer's instructions. Real-time polymerase chain reaction (PCR) was performed with a CFX96 Real-Time PCR Detection System (Bio-Rad Lab, Hercules, CA). All mRNA expression were normalized to that of GAPDH. Primers for murine GAPDH (Primer Set ID: MA050371) and Cav-1 (Primer Set ID: MA106656) were purchased from Takara Bio Inc (Shiga, Japan).

## Drugs and Solution

L-NNA, indomethacin, apamin, phenylephrine hydrochloride, acetylcholine (ACh), bradykinin (BK), and catalase were purchased from Sigma-Aldrich (St. Louis, MO), charybdotoxin from Peptide Institute (Osaka, Japan), and SNP from Maruishi Seiyaku (Osaka, Japan). The ionic composition of KHB was as follows (mmol/L); $Na^+$ 144, $K^+$ 5.9, $Mg^{2+}$ 1.2, $Ca^{2+}$ 2.5, $H_2PO^{4-}$ 1.2, $HCO^{3-}$ 24, $Cl^-$ 129.7, and glucose 5.5. The antibodies used in this study were listed in Table 3.

## Statistical Analysis

Results are expressed as mean ± SEM. Dose–response curves were analyzed by 2-way analysis of variance followed by Tukey's test for multiple comparisons. Other variables were analyzed by 2-tailed unpaired Student's *t* test. Statistical analysis was performed using GraphPad Prism version 6.00 (GraphPad Software Inc, La Jolla, CA). Results were considered to be significantly different at values of $P < 0.05$.

# RESULTS

## Endothelium-specific Deletion of Cav-1 and Caveolae

Quantitative real-time PCR to detect the gene fragments between the exon 1 and exon 3 revealed that the heart from eCav-1-KO had significantly reduced expression of the fragment (Fig. 1A). In WT controls, Cav-1 was expressed in endothelial cells, adipocytes, and to a lesser extent, in VSMCs, but not in cardiac myocytes. The expression level of Cav-1 in VSMC was comparable between the 2 genotypes. In eCav-1-KO mice, it was absent only in endothelial cells of mesenteric arteries and coronary arteries (Fig. 1B). Western blot experiments showed that both Cav-1 and Cav-2 were significantly reduced in the heart from eCav-1-KO mice, whereas Cav-3, which exists dominantly in cardiac myocytes and VSMC, was unchanged (Fig. 1C). We further analyzed the structure of the caveolae in endothelial cells and VSMC with electron microscopy. In WT controls, abundant caveolae were present in endothelial cells, whereas in eCav-1-KO mice, the caveolae were absent in endothelial cells in mesenteric arteries (Fig. 1D) and coronary microvessels (Fig. 1E). VSMC from both WT controls and eCav-1-KO mice showed only a small number of the caveolae compared with endothelial cells (Fig. 1F). Thus, we confirmed endothelium-specific Cav-1 deletion associated with endothelium-specific lack of the caveolae in eCav-1-KO mice. Coimmunoprecipitation using eNOS antibody demonstrated that Cav-1/eNOS complex was markedly decreased in mesenteric arteries in eCav-1-KO mice (Fig. 1G). Regarding eNOS activity, although the extent of eNOS phosphorylation at Ser1177 (a stimulatory site) was significantly greater in the aorta than in mesenteric artery, there was no significant difference in the phosphorylation between the 2 genotypes (Fig. 1H). By contrast, the extent of eNOS phosphorylation at Thr495 (an inhibitory site) was significantly greater in mesenteric arteries than in the aorta and was significantly decreased in mesenteric arteries in eCav-1-KO mice (Fig. 1H).

## Cardiac Hypertrophy in eCav-1-KO Mice With Normal Blood Pressure

eCav-1-KO mice showed significantly increased left ventricle and lung weights compared with WT controls (Table 1). Echocardiography measurement confirmed that wall thickness of the interventricular septum and left ventricular posterior wall were significantly increased in eCav-1-KO compared with WT controls (Table 1). Left ventricular ejection fraction and fractional shortening were comparable between the 2 genotypes (Table 1). To further examine the cardiac hypertrophy in eCav-1-KO mice, we evaluated the gene expressions of cardiac hypertrophy markers by quantitative real-time PCR. Consistent with increased left ventricle/body weight ratio and echocardiography data, the gene expression of brain natriuretic peptide and α-myosin heavy chain in the whole heart from eCav-1-KO showed significant increases as compared to the controls (Table 1). To examine the role of endothelial Cav-1 in blood pressure regulation, we performed ambulatory blood pressure monitoring using the telemetry system. Both systolic and diastolic blood pressures were comparable throughout the day between the 2 genotypes, which was also the case for pulse pressure and heart rate (Table 2). Thus, eCav-1-KO mice had cardiac hypertrophy despite normal blood pressure.

## Enhanced NO-Mediated Responses in Conduit Artery from eCav-1-KO Mice

Systemic Cav-1-KO mice have enhanced NO-cGMP pathway.[14,22] Thus, we examined whether this is also the case in eCav-1-KO mice. We used the aorta as conduit arteries and mesenteric arteries as resistance arteries.[13,14,20,23] In the aorta, ACh-induced endothelium-dependent relaxations were significantly enhanced in eCav-1-KO compared with WT controls and were abolished in endothelium-denuded vessels, indicating that the enhanced relaxations were elicited through endothelium-dependent mechanisms (Fig. 2A). The enhanced relaxations were also markedly

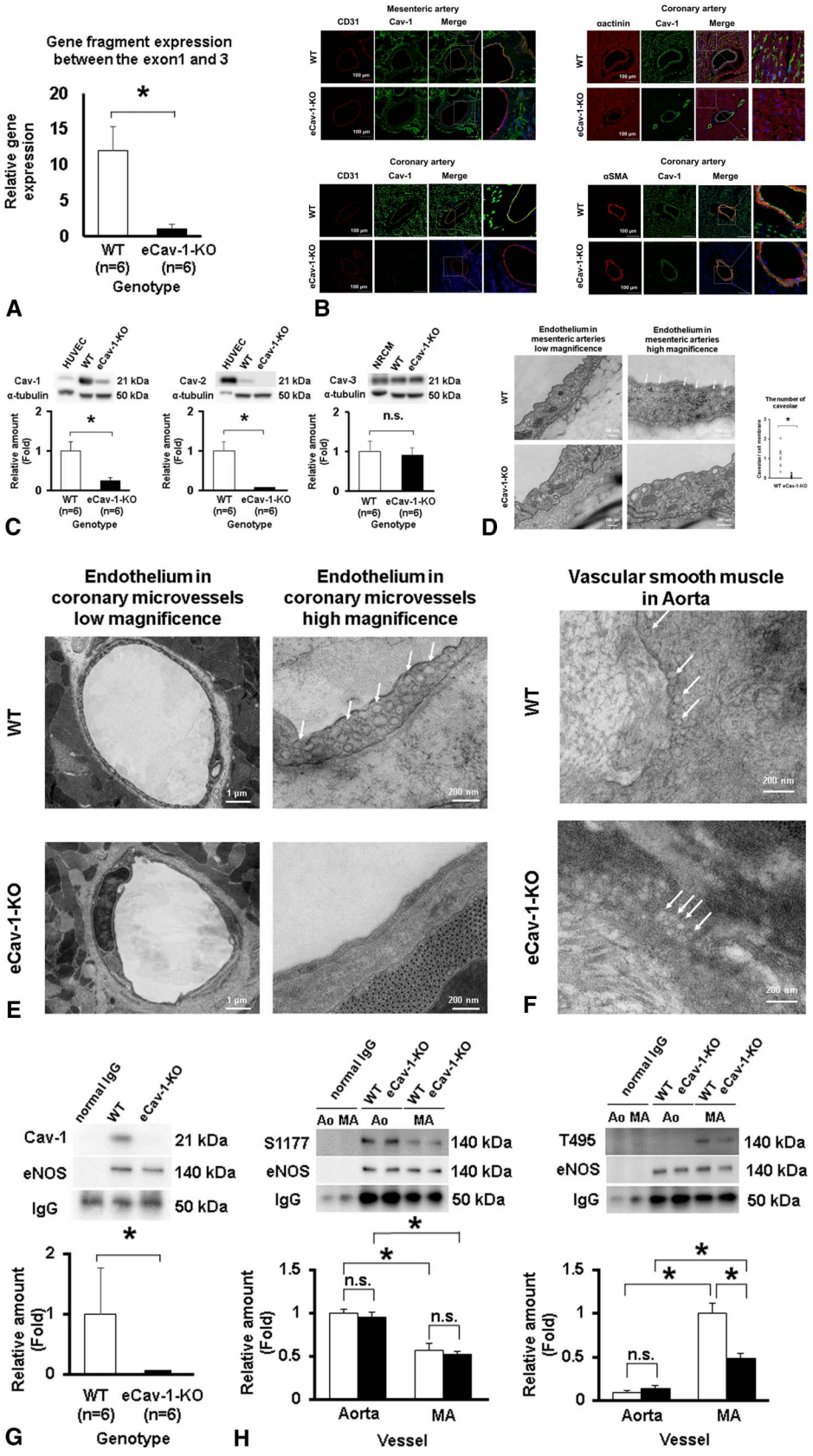


**FIGURE 1.** Characterization of eCav-1-KO mice. A, Relative mRNA expression of Cav-1 gene fragment between the exon 1 and exon 3 in the heart from WT and eCav-1-KO mice. mRNA expression was normalized to that of GAPDH. B, Immunostaining for localization of Cav-1 (green), CD31 (red), α smooth muscle actin (red), α actinin (red) and DAPI (blue) in mesenteric arteries and coronary arteries. Merged signals are shown in yellow. Scale bar, 100 μm. C, Western blot analysis of caveolin isoforms in the heart (n = 6). D, Representative images of electron microscopy of endothelial cells in mesenteric arteries and quantitative analysis of the number of the caveolae in endothelial cells (10 images from 3 mice in each genotype). E, Representative images of electron microscopy of coronary microvessels. F, Representative images of electron microscopy of vascular smooth muscle in aorta. Western blot analysis of (G) Cav-1/eNOS and (H) phosphorylated eNOS in the aorta and mesenteric arteries in coimmunoprecipitation experiment using anti-eNOS antibody (n = 6). Results are expressed as mean ± SEM. $*P < 0.05$.

**TABLE 1.** Echocardiographic Parameters and Reative mRNA Expressions

| | WT | eCav-1-KO | *P* |
|---|---|---|---|
| Organ weight (n = 8 each) | | | |
| Age (wk) | 15.2 ± 1.7 | 14.3 ± 0.7 | n.s. |
| BW (g) | 26.1 ± 1.3 | 27.0 ± 1.6 | n.s. |
| Tibia length (mm) | 17.4 ± 1.1 | 17.2 ± 0.5 | n.s. |
| Left ventricle weight (mg) | 109.1 ± 12.3 | 144.9 ± 23.9 | <0.05 |
| Left ventricle | | | |
| BW (mg/g) | 4.47 ± 0.15 | 4.82 ± 0.03 | <0.05 |
| Left ventricle | | | |
| Tibia length (mg/mm) | 6.3 ± 0.7 | 8.4 ± 1.4 | <0.05 |
| Lung (mg) | 156.6 ± 10.7 | 201.6 ± 33.4 | <0.05 |
| Lung/BW (mg/g) | 5.27 ± 0.23 | 6.21 ± 0.17 | <0.05 |
| Lung/tibia length (mg/mm) | 9.1 ± 0.8 | 11.7 ± 2.0 | <0.05 |
| Echocardiography (n = 10 each) | | | |
| IVSd (mm) | 0.79 ± 0.02 | 1.01 ± 0.02 | <0.05 |
| PWd (mm) | 0.76 ± 0.01 | 0.96 ± 0.04 | <0.05 |
| LVDd (mm) | 3.85 ± 0.09 | 3.67 ± 0.13 | n.s. |
| LVDs (mm) | 2.44 ± 0.09 | 2.31 ± 0.08 | n.s. |
| EF (%) | 66.9 ± 2.0 | 65.4 ± 1.83 | n.s. |
| FS (%) | 36.7 ± 1.52 | 35.4 ± 1.38 | n.s. |
| Relative gene expressions in ventricle (n = 7 each) | | | |
| *bnp* | 1.00 ± 0.12 | 2.70 ± 0.62 | <0.05 |
| *anp* | 1.00 ± 0.43 | 1.67 ± 0.37 | n.s. |
| *αMHC* | 1.00 ± 0.09 | 1.53 ± 0.14 | <0.05 |

Results are expressed as mean ± SEM. All mRNA expressions were normalized to those of GAPDH.

*αMHC*, alpha-myosin heavy chain; *anp*, atrial natriuretic peptide; *bnp*, brain natriuretic peptide; BW, body weight; EF, ejection fraction; FS, fractional shortening; IVSd, interventricular septal diastolic thickness; LVDd, left ventricular end-diastolic diameter; LVD, left ventricular end-systolic diameter; PWd, posterior wall diastolic thickness; WT, wild-type.

inhibited by L-NNA, indicating that NO-mediated relaxations were enhanced in eCav-1-KO mice (Fig. 2B). The relative contributions of PGs, NO, and EDH to endothelium-dependent relaxations, as evaluated by the area under the curve, also showed increased NO-mediated relaxations in eCav-1-KO mice (Fig. 2C). By contrast, basal NOS activity in eCav-1-KO mice was unaltered compared with WT controls (Fig. 2D).

## Decreased EDH-Mediated Relaxations in Resistance Arteries From eCav-1-KO Mice

In mesenteric arteries, ACh-induced endothelium-dependent relaxations were slightly but significantly decreased in eCav-1-KO compared with WT controls (Fig. 3A). Relaxation responses to ACh were resistant to indomethacin, L-NNA, or their combination in WT controls, but were highly sensitive to the combination of apamin (small conductance calcium-activated potassium channel blocker) and charybdotoxin (intermediate and large conductance calcium-activated potassium channel blocker) in the presence of indomethacin and L-NNA, indicating the primary role of EDH in mesenteric arteries (Fig. 3B). By contrast, relaxations of mesenteric arteries from eCav-1-KO mice showed enhanced NO-mediated relaxations, whereas EDH-mediated relaxations were significantly decreased (Fig. 3B, C). Basal NOS activity in mesenteric arteries was comparable between the 2 genotypes (Fig. 3D). The contribution of $H_2O_2$ in the EDH-mediated relaxation was examined by the inhibitory effect of catalase (1250 U/mL).[8,23] In the presence of both indomethacin and L-NNA, catalase markedly inhibited the relaxations in WT controls compared with eCav-1-KO mice (Fig. 3E), suggesting that endothelial production of $H_2O_2$ is markedly decreased in eCav-1-KO mice.

**TABLE 2.** Telemetric Blood Pressure Monitoring

| | WT | eCav-1-KO | *P* |
|---|---|---|---|
| Blood Pressure (n = 8 each) | | | |
| Light time | | | |
| Systolic BP (mm Hg) | 116.4 ± 5.3 | 112.1 ± 2.6 | n.s. |
| Diastolic BP (mm Hg) | 94.8 ± 4.9 | 87.9 ± 2.9 | n.s. |
| Pulse pressure (mm Hg) | 21.5 ± 1.8 | 24.2 ± 1.8 | n.s. |
| Heart rate (bpm) | 514.8 ± 29.3 | 490.6 ± 19.6 | n.s. |
| Dark time | | | |
| Systolic BP (mm Hg) | 123.2 ± 4.3 | 120.8 ± 3.4 | n.s. |
| Diastolic BP (mm Hg) | 100.0 ± 4.0 | 96.0 ± 3.1 | n.s. |
| Pulse pressure (mm Hg) | 23.3 ± 1.4 | 24.8 ± 1.9 | n.s. |
| Heart rate (bpm) | 535.3 ± 24.6 | 501.4 ± 15.3 | n.s. |

Results are expressed as mean ± SEM.

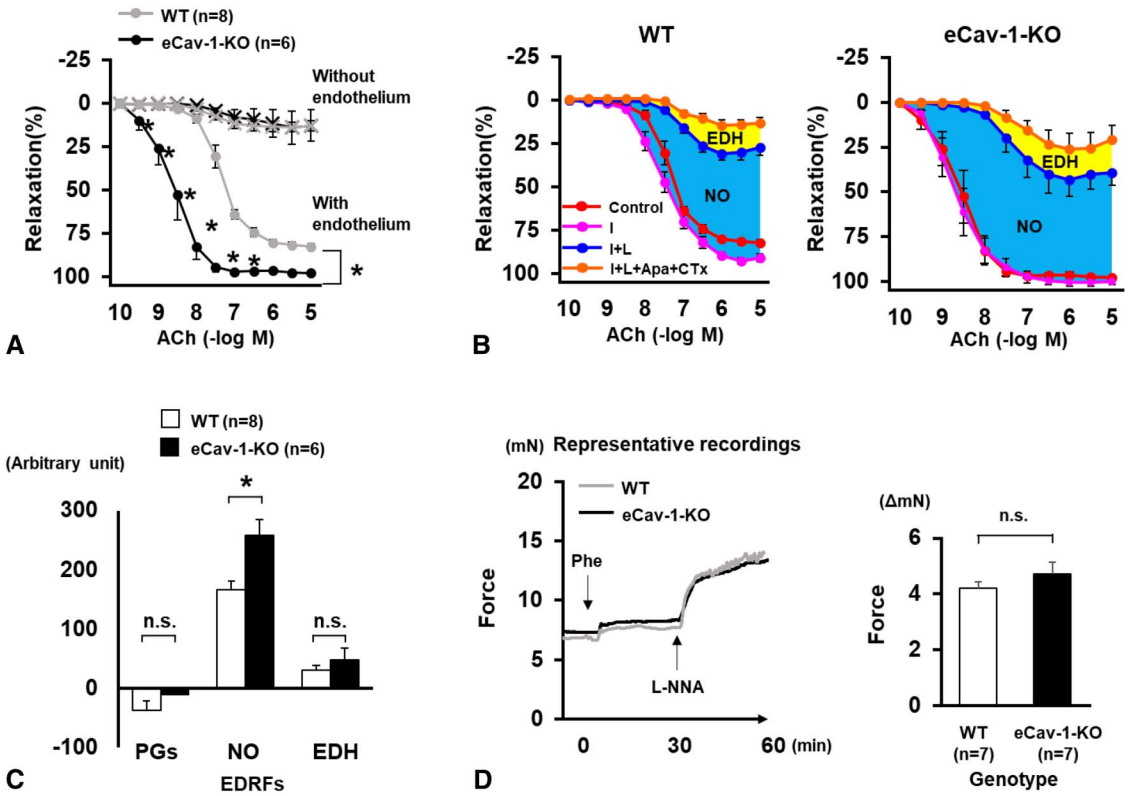


**FIGURE 2.** Enhanced NO-mediated relaxations of the aorta from eCav-1-KO mice. A, ACh-induced relaxations of the aorta from WT and eCav-1-KO mice, with and without the endothelium (n = 6–8). B and C, The contributions of vasodilator PGs (pink area), NO (blue area), and EDH (yellow area) are determined by the inhibitory effect of indomethacin, L-NNA, and a combination of charybdotoxin and apamin, respectively. The relative contributions of vasodilator PGs, NO, and EDH to endothelium-dependent relaxations were measured with area under curve (n = 6–8). D, Aortic rings were precontracted with phenylephrine and incubated with L-NNA to evaluate basal NOS activity (n = 7). Results are expressed as mean ± SEM. $*P < 0.05$.

## Decreased EDH Responses in Membrane Potentials of VSMC From eCav-1-KO Mice

Although resting membrane potentials of VSMC in mesenteric arteries were comparable between the 2 genotypes (Fig. 3F, G), hyperpolarization responses to ACh in the presence of indomethacin and L-NNA were significantly decreased in eCav-1-KO mice compared with WT controls (Fig. 3F, H).

## Endothelium-independent Relaxations

Endothelium-independent responses of VSMC of the aorta and mesenteric arteries to a NO donor SNP (Fig. 4A, B) and a K channel opener NS-1619 (Fig. 4C, D) were comparable between the 2 genotypes. VSMC responses to exogenous $H_2O_2$, a major EDH-mediated factor in mouse mesenteric arteries,[8–10] were also comparable between the 2 genotypes (Fig. 4E, F).

## Coronary Flow Responses in Isolated Langendorff-Perfused Heart

In this experiment, as heart weight was different between the 2 genotypes, all coronary flow values were normalized to heart weight. In the perfused heart, baseline coronary flow was significantly higher in eCav-1-KO compared with WT controls (Fig. 5A, B). Coronary flow in response to BK was also significantly higher in eCav-1-KO compared with control mice (Fig. 5B, C). By contrast, no significant difference in endothelium-independent response to SNP or adenosine was noted between the 2 genotypes (Fig. 5B). The increased coronary flow response to BK in eCav-1-KO mice was abolished by L-NNA, suggesting that NO-mediated response was enhanced (Fig. 5D, E). In the presence of L-NNA and indomethacin (EDH condition), coronary flow increase to BK was significantly reduced in eCav-1-KO compared with WT controls (Fig. 5F–H).

## Evidence for Nitrative Stress in the Heart From eCav-1-KO Mice

eNOS expression in the heart from eCav-1-KO mice was significantly higher compared with WT controls (Fig. 6A). In eCav-1-KO mice compared with WT control, cardiac eNOS phosphorylation at stimulatory Ser1177 site was comparable (Fig. 6B), whereas that at inhibitory Thr495 site was significantly decreased (Fig. 6C), a consistent finding with mesenteric arteries. The concentration of cardiac cyclic GMP was significantly higher in eCav-1-KO compared with WT controls, indicating the enhanced NO-cGMP pathway in the heart from eCav-1-KO mice (Fig. 6D). We also measured

**TABLE 3.** Antibodies for Western Blotting and Immunocytochemistry

| Antibody | Company | Catalog Number |
|---|---|---|
| α actinin | Abcam | #ab9465 |
| α smooth muscle actin | Sigma | #C6198 |
| Caveolin-1 | Cell Signaling Technology | #3267 |
| Caveolin-2 | Cell Signaling Technology | #8522 |
| Caveolin-3 | Abcam | #ab2912 |
| eNOS | BD Transduction Laboratories | #610296 |
| p-eNOS (S1177) | BD Transduction Laboratories | #612393 |
| p-eNOS (T495) | BD Transduction Laboratories | #9574 |
| ERK1/2 | Cell Signaling Technology | #9102 |
| p-ERK1/2 (T202/Y204) | Cell Signaling Technology | #9101 |
| α-tubulin | Sigma | #T9026 |
| p38MAPK | Cell Signaling Technology | #9212 |
| p-p38MAPK (T180/Y182) | Cell Signaling Technology | #9211 |
| JNK | Cell Signaling Technology | #9252 |
| p-JNK (T183/Y185) | Cell Signaling Technology | #9251 |
| PI3 kinase | Cell Signaling Technology | #5405 |
| CD31 | BD Pharmingen | #550274 |
| H-Ras | Abcam | #Y132 |

the concentration of 3-nitrotyrosine (3-NT) in the heart as a footprint of peroxynitrite by enzyme-linked immunosorbent assay.[24] The 3-NT levels in the heart were comparable between the 2 genotypes (Fig. 6E). Recently, the formation of 8-nitroguanosine 3, 5-cyclic monophosphate (8-nitro-cGMP) in a NO-dependent manner has been reported as a nitrative stress.[25] Immunohistochemical staining showed that enhanced immunoreactivity of cardiac 8-nitro-cGMP was evident in eCav-1-KO mice (Fig. 6F). 8-Nitro-cGMP can form protein Cys-cGMP adducts as a posttranslational modification, which is called protein S-guanylation.[25] 8-nitro-cGMP selectively targets an oncogenic small GTPase H-Ras, leading to cardiac senescence by S-guanylation and activation of H-Ras.[26] In this study, we confirmed that exogenous 8-nitro-cGMP caused S-guanylation of cardiac H-Ras in a dose-dependent manner (Fig. 6G). Endogenous S-guanylation of cardiac H-Ras was detected in nonreduced condition, but not in reduced condition, in both genotypes (Fig. 6H). The extent of S-guanylation of cardiac H-Ras was significantly increased in eCav-1-KO compared with WT controls in nonreduced condition (Fig. 6H). An important downstream cellular response to Ras activation is mediated by MAP kinase and phosphatidylinositol-3-kinase (PI3K).[27] The hearts from eCav-1-KO mice showed that ERK was significantly activated, p38 significantly suppressed, and JNK and PI3K unaltered (Fig. 6I).

## DISCUSSION

The novel findings of this study with eCav-1-KO mice were that (1) endothelium-specific deletion of Cav-1 caused enhancement of NO-cGMP pathway and suppression of EDH-mediated responses in resistance vessels, (2) the excessive NO-mediated responses caused coronary microcirculatory dysfunction and cardiac hypertrophy, and (3) enhanced nitrative stress by 8-nitro-cGMP may be involved in those pathological changes (Fig. 7).

### Endothelium-Specific Deletion of Cav-1 Enhances NO-Mediated Responses

One of the regulatory mechanisms of eNOS activity is phosphorylation at stimulatory Ser1177 site, which is independent of an increase in $Ca^{2+}$ or agonist stimulation, followed by mild increase in NO production.[28] However, in this study, the extent of eNOS phosphorylation at Ser1177 was comparable between eCav-1-KO and WT controls. This may explain why basal NO release was comparable between the 2 genotypes. By contrast, agonist-induced and $Ca^{2+}$-dependent activation of eNOS is mainly associated with dephosphorylation at inhibitory Thr495 site in the CaM-binding domain, resulting in burst NO increase.[28] In this study, the extent of eNOS phosphorylation at Thr495 was significantly reduced in both mesenteric arteries and the heart from eCav-1-KO mice compared with WT controls, resulting in high sensitivity to agonist stimulation and enhanced NO-mediated responses. Several receptors including ACh and BK receptors are located in the caveolae. Although physiological NO release requires eNOS in the caveolae, eNOS activation may not necessarily require eNOS itself in the caveolae.[29] In addition, previous studies have reported the enhanced agonist-induced eNOS activation in systemic Cav-1-KO mice.[14,22] Thus, the enhanced agonist-induced NO responses in eCav-1-KO can be attributable to the loss of the direct allosteric inhibitory effect of Cav-1 on eNOS.

In general, $Ca^{2+}$ entry pathways including voltage-gated $Ca^{2+}$ channels and transient receptor potential channels are localized in the caveolae.[30] It is possible that the disappearance of endothelial caveolae along with the deletion of eCav-1 may affect the mechanism of intracellular $Ca^{2+}$ entry into endothelial cells, followed by the changes in eNOS phosphorylation at Thr495 that is partly regulated by intracellular $Ca^{2+}$ concentration.

### Endothelial Cav-1 Regulates EDH Responses in Resistance Arteries

In eCav-1-KO mice, NO-mediated relaxations were enhanced in both the aorta and mesenteric arteries, whereas EDH-mediated relaxations were reduced in mesenteric arteries. Recently, we have reported that systemic Cav-1-KO mice showed enhanced NO-mediated relaxations and decreased EDH-mediated relaxations.[13,14] The present findings are consistent with those results, demonstrating the crucial roles of endothelial Cav-1 in EDH-mediated responses. We have previously demonstrated that eNOS-derived $H_2O_2$ is an EDH factor in mouse mesenteric arteries.[8] In eCav-1-KO mice, the Cav-1/eNOS complex and eNOS phosphorylation at Thr495 were markedly reduced in mesenteric arteries, indicating dysregulation of eNOS in those mice. NOSs have been known to generate superoxide anions from reductase domain

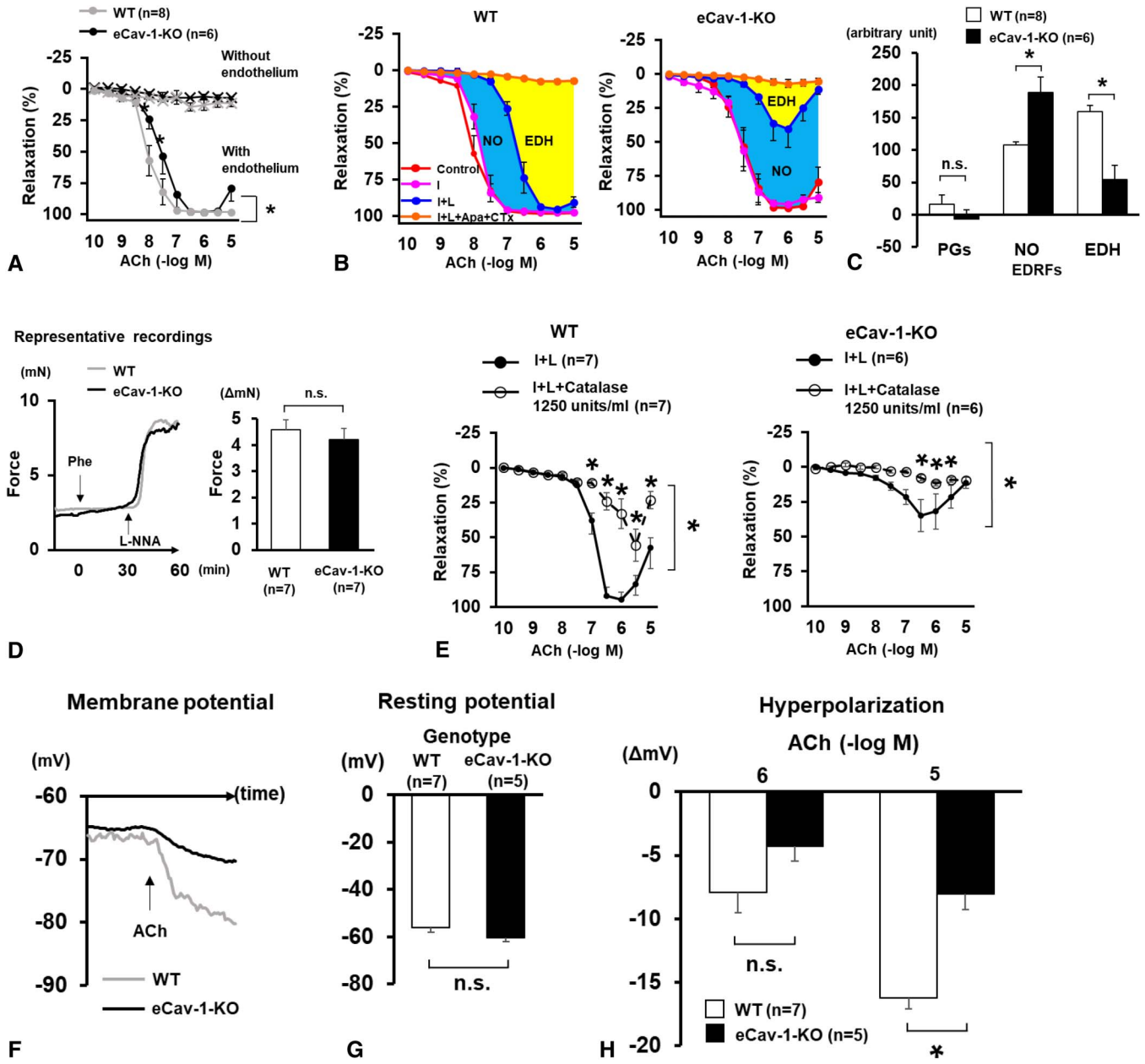


**FIGURE 3.** Reduced EDH-mediated relaxations in mesenteric arteries from eCav-1-KO mice. A, ACh-induced relaxations of mesenteric artery from WT and eCav-1-KO mice, with and without the endothelium (n = 6–8). B and C, The relative contributions of vasodilator PGs, NO, and EDH to endothelium-dependent relaxations (n = 6–8). D, Basal NOS activity. E, The inhibitory effect of Catalase (1250 units/mL) on EDH-mediated relaxations in mesenteric artery (n = 6–7). F, Representative membrane potential recordings, (G) quantitative analysis of resting potentials, and (H) hyperpolarization to ACh of VSMC in mesenteric arteries (n = 5–7). Results are expressed as mean ± SEM. *$P < 0.05$.

under physiological conditions, where superoxide anions are converted into $H_2O_2$ to cause EDH-mediated responses.[9,10,12] However, NO generation in eNOS requires an electron trans2fer from reductase domain to oxygenase domain.[31] It has been reported that Cav-1 can compromise the electron transfer from the reductase domain to the oxygenase domain and inhibit NO generation.[32] Thus, we consider that the deletion of endothelial Cav-1 may increase the amount of electron from reductase domain to oxygenase domain in eNOS, resulting in the enhanced NO synthesis. Conversely, the amount of electron decreases in reductase domain, followed by the attenuated generation of superoxide anions, and consequently decreased $H_2O_2$ in eCav-1-KO.

In this study, catalase-sensitive relaxations, that is, $H_2O_2$-mediated relaxations, were markedly decreased in eCav-1-KO mice, indicating the importance of eNOS/Cav-1 complex in producing $H_2O_2$/EDH factor.

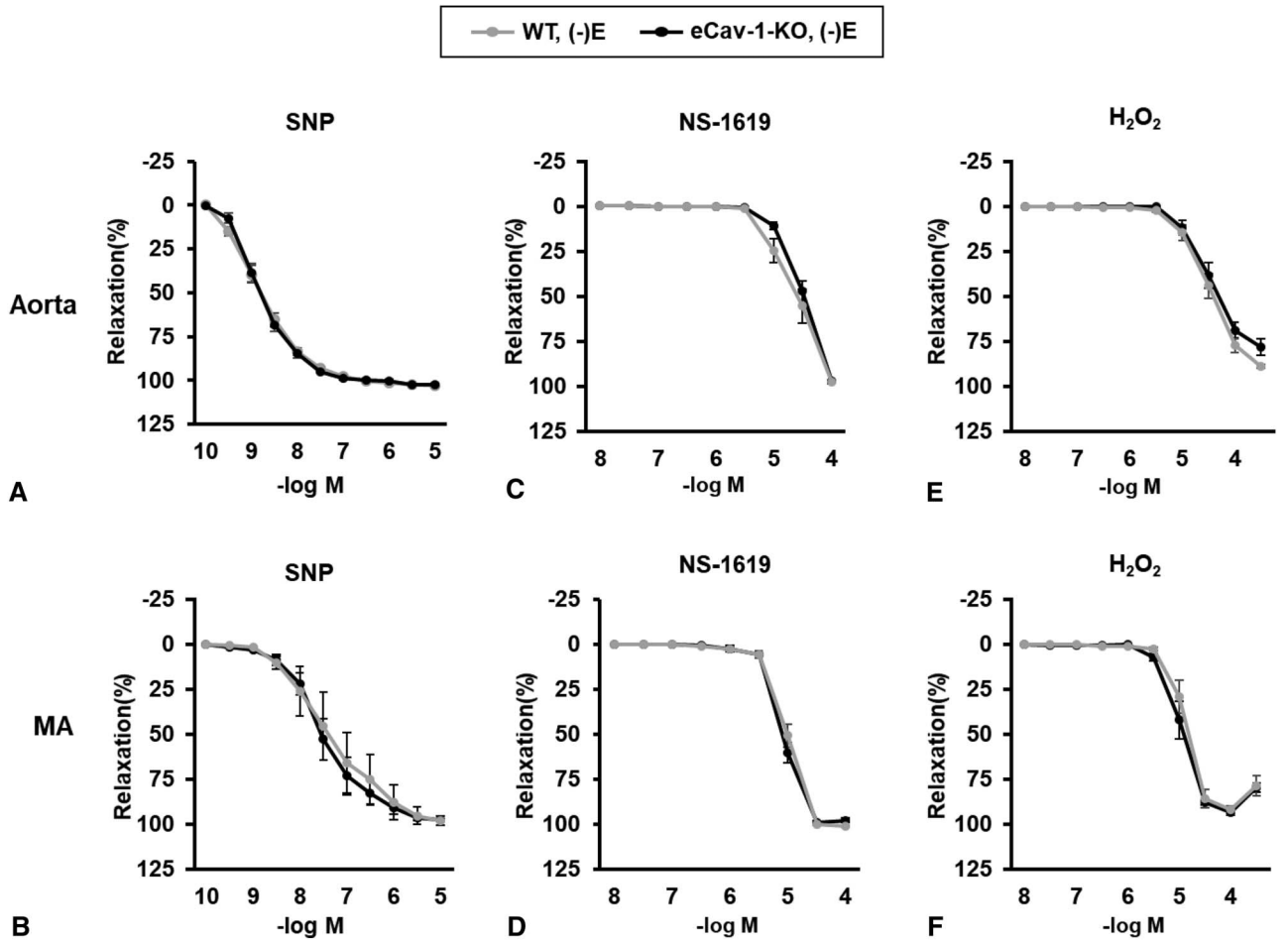


**FIGURE 4.** Endothelium-independent relaxations. Endothelium-independent relaxations of the aorta and mesenteric arteries to SNP (A and B) and NS-1619 (C and D). The responses to $H_2O_2$ were examined in the presence of indomethacin ($10^{-5}$ mol/L) and L-NNA ($10^{-4}$ mol/L) (E and F) (n = 4). Relaxations were examined in rings without endothelium. Results are expressed as mean ± SEM.

## Endothelial Cav-1 Regulates Coronary Microcirculation

In this study, we also examined the physiological significance of endothelial Cav-1 in coronary microcirculation by using Langendorff-perfused heart. Baseline coronary flow was significantly increased in eCav-1-KO mice compared with WT controls. The increase in baseline coronary flow in eCav-1-KO mice was abolished by L-NNA, indicating the enhanced contribution of NO to baseline coronary flow. Furthermore, eCav-1-KO mice showed enhanced NO-mediated coronary responses to BK. By contrast, EDH-mediated responses of coronary microcirculation were decreased in eCav-1-KO mice. These findings in Langendorff-perfused hearts were consistent with those in isometric tension experiments showing enhanced NO-mediated responses and decreased EDH-mediated responses in mesenteric arteries. The importance of EDH-mediated responses in coronary microcirculation has been repeatedly reported. In the canine coronary microcirculation in vivo, endothelium-derived $H_2O_2$ as an EDH factor plays an important role in coronary autoregulation,[33] myocardial protection against ischemia/reperfusion injury,[34] and metabolic coronary dilatation.[35] Also in human coronary arterioles, endothelium-derived $H_2O_2$ plays an important role in flow-induced dilatation.[36] Although eCav-1-KO mice showed spontaneous development of cardiac hypertrophy, systolic functions evaluated by echocardiography were maintained in this study. Because we used relatively young mice for echocardiography experiment, it could be possible that systolic functions may be altered at advanced age. Further studies are needed to clarify the long-term influence of dysregulated coronary microcirculation on cardiac function at advanced age.

## Excessive eNOS-Derived NO Causes Nitrative Stress With 8-Nitro-cGMP

In this study, endothelium-specific deletion of Cav-1 caused enhanced NO responses and reduced EDH responses with spontaneous development of cardiac hypertrophy in mice despite normal blood pressure. It has been previously reported that systemic blood pressure is unchanged in systemic Cav-1-KO mice despite increased NO production.[14,37,38] The present findings with eCav-1-KO mice are

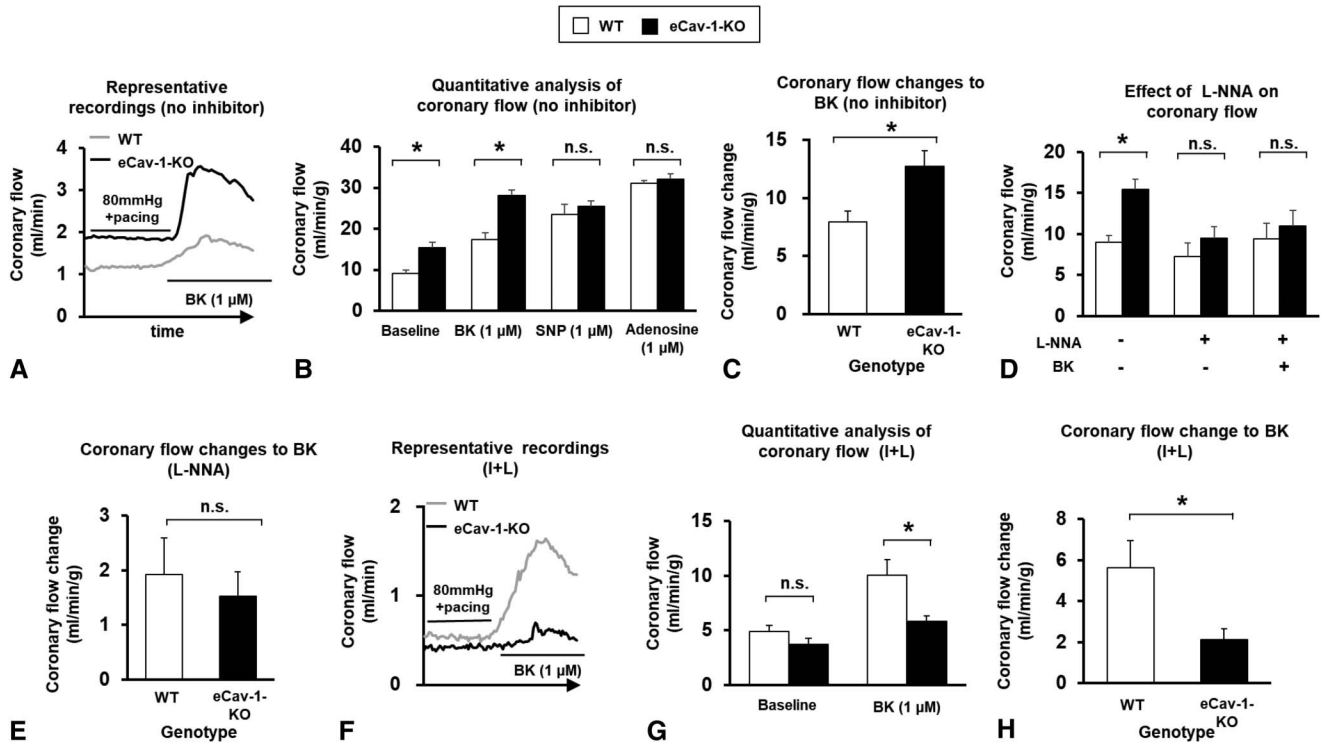


**FIGURE 5.** Coronary flow responses in isolated Langendorff-perfused heart. A, Representative recordings and (B) quantitative analysis of coronary flow in response to BK (n = 5), SNP (n = 4) and adenosine (n = 5). C, Coronary flow changes to BK (n = 5). D and E, Effects of L-NNA on coronary flow responses (n = 4–5). F, Representative recordings and (G) quantitative analysis of coronary flow in response to BK in the presence of indomethacin and L-NNA (n = 5–6). H, Coronary flow changes to BK in the presence of indomethacin and L-NNA. Results are expressed as mean ± SEM. $*P < 0.05$.

consistent with these findings, suggesting that the activation of eNOS due to the lack of Cav-1 may not cause hypotension. A previous study demonstrated that endothelium-specific Cav-1 reconstitution improved vasomotion and cardiac and pulmonary abnormalities in systemic Cav-1-KO mice.[39] These findings are consistent with this study, suggesting a primary role for endothelial Cav-1 in the pathogenesis of cardiac hypertrophy. It also has been reported that systemic Cav-1-KO mice at advanced age show pulmonary hypertension and reduced life span.[40,41] eCav-1-KO mice showed increased lung weight, indicating the pulmonary abnormalities as seen in systemic Cav-1-KO mice. Further studies are needed to clarify the pulmonary abnormalities including pulmonary hypertension in eCav-1-KO mice.

In general, high NO production by iNOS has adverse effects in some inflammatory diseases,[42] whereas endothelial production of physiological levels of NO by eNOS is cardioprotective.[43] NO causes vascular relaxation mainly through cGMP-dependent mechanism especially in conduit arteries;[6,44] however, it is conceivable that pathways other than NO-cGMP signalings are involved in some NO-mediated signalings in various cells and tissues. In eCav-1-KO mice, eNOS-derived excessive NO could cause adverse cardiac changes without affecting eNOS uncoupling or peroxynitrite levels. It has recently been demonstrated that 8-nitro-cGMP, a novel nitrated cyclic nucleotide, is generated through excessive NO.[25] In this study, immunoreactivity of 8-nitro-cGMP was enhanced in the heart from eCav-1-KO mice as nitrative stress. 8-nitro-cGMP has strong redox activity and reacts with sulfhydryl groups of cysteine residues and forms protein S-cGMP adduct through a posttranslational modification, which is named as protein S-guanylation.[25] It has been reported that a cysteine residue of an oncogenic small GTPase H-Ras is one of the selective targets of S-guanylation.[26] S-guanylation-dependent activation of H-Ras causes ERK activation and plays an important role in cardiac cell senescence in mouse cardiac tissues.[26] In addition, ERK is known to play a central role in cardiac hypertrophy.[27,45] The present results are consistent with these findings, indicating that activation of H-Ras-ERK pathway is involved in the pathogenesis of cardiac hypertrophy in eCav-1-KO.

In this study, we were able to detect endogenous S-guanylation of cardiac H-Ras in nonreduced condition but not in reduced condition. Reactive sulfur intermediates, such as hydropersulfides (RSSH) and polysulfides [$RS(S)_nH$ and $RS(S)_nSR$] are formed during sulfur-containing amino acid metabolism and have critical regulatory functions in redox cell signaling mediated by 8-nitro-cGMP.[46] The present results indicate that cysteine reactive sulfur intermediates in cardiac H-Ras mainly mediate redox signaling through S-guanylation. However, eNOS is also sensitive to oxidative protein modification such as S-glutathionylation and S-nitrosylation at its cysteine residues. Considering the biochemical characteristics of eNOS, it is possible that S-guanylation can regulate eNOS

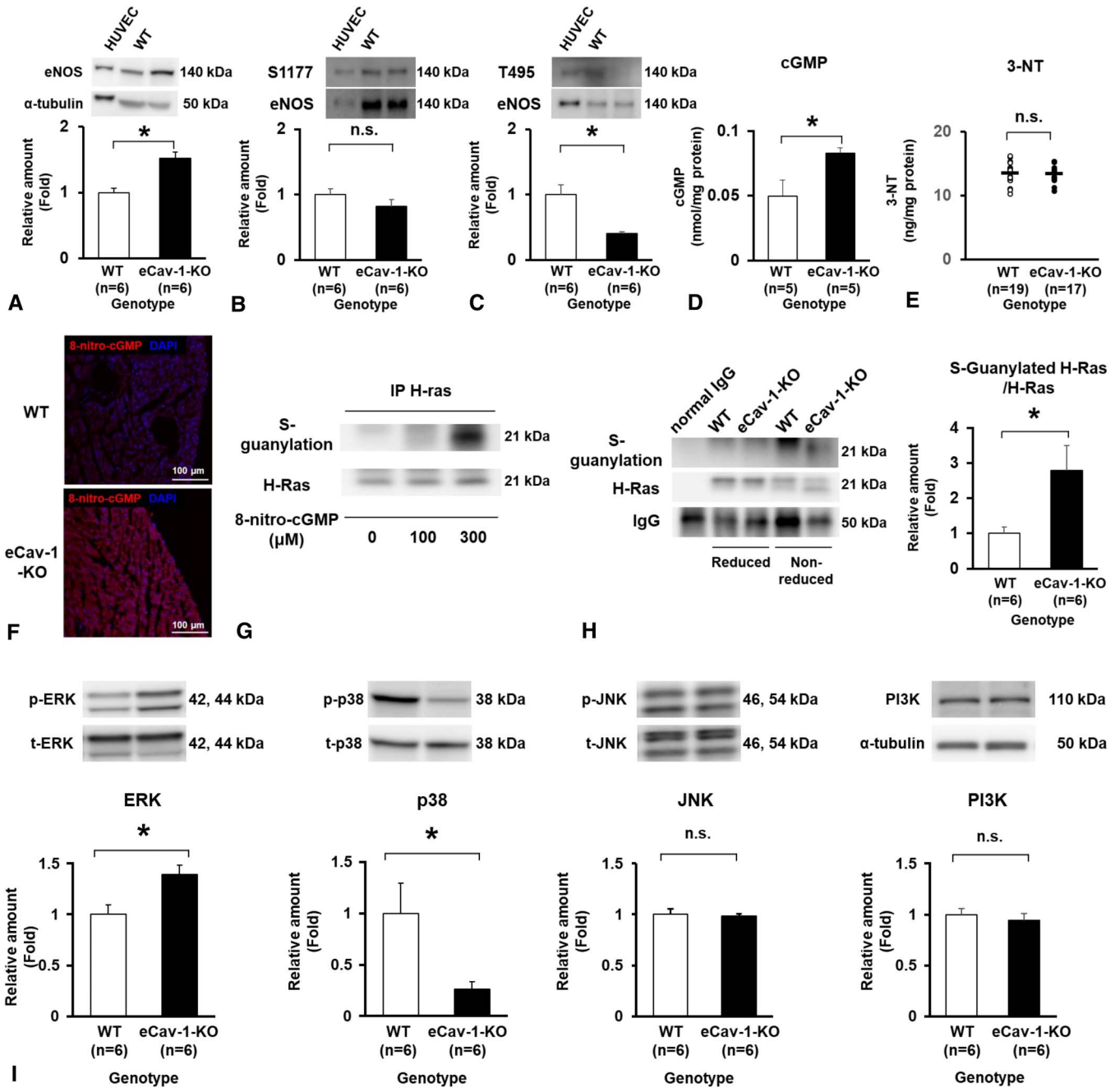


**FIGURE 6.** Enhanced NO-cGMP pathway and 8-nitro-cGMP formation. Western blot analysis of (A) eNOS, (B, C) phosphorylated eNOS in the heart (n = 6). D, Cardiac cGMP concentration (n = 5). F, Representative staining of 8-nitro-cGMP. G, S-guanylation of cardiac H-Ras caused by exogenous 8-nitro-cGMP. H, Western blot analysis of endogenous S-guanylation of cardiac H-Ras in coimmunoprecipitation experiment using anti-H-Ras antibody (n = 6). I, Western blot analysis in whole heart lysates of ERK, p38, JNK, and PI3K. Results are expressed as mean ± SEM. $*P < 0.05$.

function in eCav-1-KO mice. Further studies are needed to clarify the role of S-guanylation in regulating the function of eNOS.

## Perspectives

In this study, endothelium-specific Cav-1 deletion caused cardiac hypertrophy. These findings suggest that EDRFs can modulate not only cardiac microvascular circulation but also homeostasis of adjacent cardiac tissues including cardiac myocyte. Considering the fact that the present findings has shown that excessive NO impairs cardiac microcirculation and causes cardiac hypertrophy, it is conceivable that the physiological balance between NO and EDH plays important role in maintaining cardiovascular homeostasis.

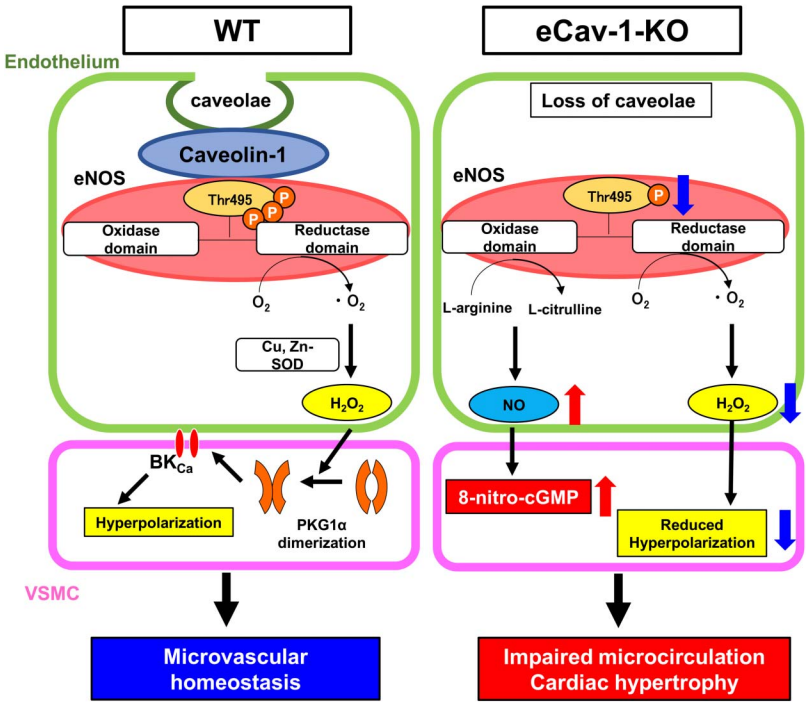


**FIGURE 7.** Summary of this study. Cav-1 is involved in enhanced EDH-mediated responses in microcirculation through functional inhibition of eNOS. Endothelium-specific Cav-1 deletion results in disappearance of the caveolae in the endothelium, causing eNOS activation followed by excessive NO production and attenuated EDH response. Excessive NO generates 8-nitro-cGMP as one of the nitrative stress in the heart, causing S-guanylation of cardiac H-Ras and consequent cardiac hypertrophy.

## Study Limitations

Several limitations should be mentioned for this study. First, although we used Tie2 as a driver for endothelial cell expression in this study, it is known that Tie2 is also expressed in hematopoietic lineages.[47] Thus, we need to consider the possible involvement of hematopoietic cells in the phenotype of Tie2-promoter–dependent Cav-1-KO mice. Second, it has been proposed that myoendothelial gap junctions play important roles for EDH-mediated responses involving endothelial Ca-activated potassium channels.[48] Potassium channels and gap junctions are located in caveolae and are regulated by Cav-1[49] and not only eCav-1 but also caveolae structure were absent in eCav-1-KO mice. Thus, eCav-1-KO mice are likely to have some other abnormalities regarding myoendothelial gap junctions that were not documented in this study. Third, the mechanism of the enhanced eNOS expression in eCav-1-KO mice remains to be elucidated. It has been reported that systemic Cav-1-KO mice have increased undifferentiated vessels with a resultant enhanced proportion of endothelial cells.[22] Thus, this also could be the case with eCav-1-KO mice in this study. Fourth, to address the role of EDH in microvessels, we used the experimental approach to inhibit EDH responses by enhancing NO-mediated responses in this study. Thus, another experimental approach to enhance EDH responses remains to be examined. However, our preliminary experiments showed that it is difficult to further enhance EDH responses in microvessels (eg, endothelium-specific overexpression of Cav-1). Finally, the cause-and-effect relationship between enhanced production of 8-nitro-cGMP and cardiac hypertrophy remains to be further elucidated.

## CONCLUSIONS

These results suggest that excessive NO impairs cardiac microvascular homeostasis through nitrative stress caused by 8-nitro-cGMP, indicating the protective role of EDH against excessive NO, for which eCav-1 is substantially involved.

## ACKNOWLEDGMENTS

*The authors appreciate Y. Watanabe, H. Yamashita, and A. Nishihara for their excellent technical assistance.*

## REFERENCES

1. Shimokawa H. 2014 Williams Harvey Lecture: importance of coronary vasomotion abnormalities-from bench to bedside. *Eur Heart J.* 2014;35:3180–3193.
2. Busse R, Edwards G, Feletou M, et al. EDHF: bringing the concepts together. *Trends Pharmacol Sci.* 2002;23:374–380.
3. Feletou M, Vanhoutte PM. Endothelium-derived hyperpolarizing factor: where are we now? *Arterioscler Thromb Vasc Biol.* 2006;26:1215–1225.
4. Feletou M, Vanhoutte PM. Endothelium-dependent hyperpolarization of canine coronary smooth muscle. *Br J Pharmacol.* 1988;93:515–524.
5. Chen G, Suzuki H, Weston AH. Acetylcholine releases endothelium-derived hyperpolarizing factor and EDRF from rat blood vessels. *Br J Pharmacol.* 1988;95:1165–1174.
6. Shimokawa H, Yasutake H, Fujii K, et al. The importance of the hyperpolarizing mechanism increases as the vessel size decreases in endothelium-dependent relaxations in rat mesenteric circulation. *J Cardiovasc Pharmacol.* 1996;28:703–711.
7. Urakami-Harasawa L, Shimokawa H, Nakashima M, et al. Importance of endothelium-derived hyperpolarizing factor in human arteries. *J Clin Invest.* 1997;100:2793–2799.
8. Matoba T, Shimokawa H, Nakashima M, et al. Hydrogen peroxide is an endothelium-derived hyperpolarizing factor in mice. *J Clin Invest.* 2000;106:1521–1530.
9. Matoba T, Shimokawa H, Kubota H, et al. Hydrogen peroxide is an endothelium-derived hyperpolarizing factor in human mesenteric arteries. *Biochem Biophys Res Commun.* 2002;290:909–913.
10. Matoba T, Shimokawa H, Morikawa K, et al. Electron spin resonance detection of hydrogen peroxide as an endothelium-derived hyperpolarizing factor in porcine coronary microvessels. *Arterioscler Thromb Vasc Biol.* 2003;23:1224–1230.

11. Takaki A, Morikawa K, Tsutsui M, et al. Crucial role of nitric oxide synthases system in endothelium-dependent hyperpolarization in mice. *J Exp Med.* 2008;205:2053–2063.
12. Morikawa K, Shimokawa H, Matoba T, et al. Pivotal role of Cu,Zn-superoxide dismutase in endothelium-dependent hyperpolarization. *J Clin Invest.* 2003;112:1871–1879.
13. Ohashi J, Sawada A, Nakajima S, et al. Mechanisms for enhanced endothelium-derived hyperpolarizing factor-mediated responses in microvessels in mice. *Circ J.* 2012;76:1768–1779.
14. Godo S, Sawada A, Saito H, et al. Disruption of physiological balance between nitric oxide and endothelium-dependent hyperpolarization impairs cardiovascular homeostasis in mice. *Arterioscler Thromb Vasc Biol.* 2016;36:97–107.
15. Scherer PE, Lewis RY, Volonte D, et al. Cell-type and tissue-specific expression of caveolin-2. Caveolins 1 and 2 co-localize and form a stable hetero-oligomeric complex in vivo. *J Biol Chem.* 1997;272:29337–29346.
16. Way M, Parton RG. M-caveolin, a muscle-specific caveolin-related protein. *FEBS Lett.* 1995;376:108–112.
17. Razani B, Engelman JA, Wang XB, et al. Caveolin-1 null mice are viable but show evidence of hyperproliferative and vascular abnormalities. *J Biol Chem.* 2001;276:38121–38138.
18. Galbiati F, Volonte D, Engelman JA, et al. Targeted downregulation of caveolin-1 is sufficient to drive cell transformation and hyperactivate the p42/44 map kinase cascade. *EMBO J.* 1998;17:6633–6648.
19. Bernatchez P, Sharma A, Bauer PM, et al. A noninhibitory mutant of the caveolin-1 scaffolding domain enhances eNOS-derived NO synthesis and vasodilation in mice. *J Clin Invest.* 2011;121:3747–3755.
20. Enkhjargal B, Godo S, Sawada A, et al. Endothelial AMP-activated protein kinase regulates blood pressure and coronary flow responses through hyperpolarization mechanism in mice. *Arterioscler Thromb Vasc Biol.* 2014;34:1505–1513.
21. Suzuki K, Satoh K, Ikeda S, et al. Basigin promotes cardiac fibrosis and failure in response to chronic pressure overload in mice. *Arterioscler Thromb Vasc Biol.* 2016;36:636–646.
22. Drab M, Verkade P, Elger M, et al. Loss of caveolae, vascular dysfunction, and pulmonary defects in caveolin-1 gene-disrupted mice. *Science*. 2001;293:2449–2452.
23. Nakajima S, Ohashi J, Sawada A, et al. Essential role of bone marrow for microvascular endothelial and metabolic functions in mice. *Circ Res.* 2012;111:87–96.
24. Oyama J, Shimokawa H, Momii H, et al. Role of nitric oxide and peroxynitrite in the cytokine-induced sustained myocardial dysfunction in dogs in vivo. *J Clin Invest.* 1998;101:2207–2214.
25. Sawa T, Zaki MH, Okamoto T, et al. Protein S-guanylation by the biological signal 8-nitroguanosine 3′,5′-cyclic monophosphate. *Nat Chem Biol.* 2007;3:727–735.
26. Nishida M, Sawa T, Kitajima N, et al. Hydrogen sulfide anion regulates redox signaling via electrophile sulfhydration. *Nat Chem Biol.* 2012;8:714–724.
27. Gelb BD, Tartaglia M. Ras signaling pathway mutations and hypertrophic cardiomyopathy: getting into and out of the thick of it. *J Clin Invest.* 2011;121:844–847.
28. Fleming I, Fisslthaler B, Dimmeler S, et al. Phosphorylation of $Thr^{495}$ regulates $Ca^{2+}$/calmodulin-dependent endothelial nitric oxide synthase activity. *Circ Res.* 2001;88:E68–E75.
29. Sowa G, Pypaert M, Sessa WC. Distinction between signaling mechanisms in lipid rafts vs. caveolae. *Proc Natl Acad Sci U S A.* 2001;98:14072–14077.
30. Pani B, Singh BB. Lipid rafts/caveolae as microdomains of calcium signaling. *Cell Calcium*. 2009;45:625–633.
31. Stuehr D, Pou S, Rosen GM. Oxygen reduction by nitric-oxide synthases. *J Biol Chem.* 2001;276:14533–14536.
32. Ghosh S, Gachhui R, Crooks C, et al. Interaction between caveolin-1 and the reductase domain of endothelial nitric-oxide synthase. Consequences for catalysis. *J Biol Chem.* 1998;273:22267–22271.
33. Yada T, Shimokawa H, Hiramatsu O, et al. Hydrogen peroxide, an endogenous endothelium-derived hyperpolarizing factor, plays an important role in coronary autoregulation in vivo. *Circulation*. 2003;107:1040–1045.
34. Yada T, Shimokawa H, Hiramatsu O, et al. Cardioprotective role of endogenous hydrogen peroxide during ischemia-reperfusion injury in canine coronary microcirculation in vivo. *Am J Physiol Heart Circ Physiol.* 2006;291:H1138–H1146.
35. Yada T, Shimokawa H, Hiramatsu O, et al. Important role of endogenous hydrogen peroxide in pacing-induced metabolic coronary vasodilation in dogs in vivo. *J Am Coll Cardiol.* 2007;50:1272–1278.
36. Miura H, Bosnjak JJ, Ning G, et al. Role for hydrogen peroxide in flow-induced dilation of human coronary arterioles. *Circ Res.* 2002;92:e31–e40.
37. Desjardins F, Lobysheva I, Pelat M, et al. Control of blood pressure variability in caveolin-1-deficient mice: role of nitric oxide identified in vivo through spectral analysis. *Cardiovasc Res.* 2008;79:527–536.
38. Dessy C, Feron O, Balligand JL. The regulation of endothelial nitric oxide synthase by caveolin: a paradigm validated in vivo and shared by the "endothelium-derived hyperpolarizing factor". *Pflugers Arch.* 2010;459:817–827.
39. Murata T, Lin MI, Huang Y, et al. Reexpression of caveolin-1 in endothelium rescues the vascular, cardiac, and pulmonary defects in global caveolin-1 knockout mice. *J Exp Med.* 2007;204:2373–2382.
40. Park DS, Cohen AW, Frank PG, et al. Caveolin-1 null (-/-) mice show dramatic reductions in life span. *Biochemistry*. 2003;42:15124–15131.
41. Zhao YY, Liu Y, Stan RV, et al. Defects in caveolin-1 cause dilated cardiomyopathy and pulmonary hypertension in knockout mice. *Proc Natl Acad Sci U S A.* 2002;99:11375–11380.
42. Clancy RM, Amin AR, Abramson SB. The role of nitric oxide in inflammation and immunity. *Arthritis Rheum.* 1998;41:1141–1151.
43. Forstermann U, Closs EI, Pollock JS, et al. Nitric oxide synthase isozymes. Characterization, purification, molecular cloning, and functions. *Hypertension*. 1994;23:1121–1131.
44. Murad F. Cyclic guanosine monophosphate as a mediator of vasodilation. *J Clin Invest.* 1986;78:1–5.
45. Ruwhof C, van der Laarse A. Mechanical stress-induced cardiac hypertrophy: mechanisms and signal transduction pathways. *Cardiovasc Res.* 2000;47:23–37.
46. Ida T, Sawa T, Ihara H, et al. Reactive cysteine persulfides and S-polythiolation regulate oxidative stress and redox signaling. *Proc Natl Acad Sci U S A.* 2014;111:7606–7611.
47. Kisanuki YY, Hammer RE, Miyazaki J, et al. Tie2-Cre transgenic mice: a new model for endothelial cell-lineage analysis in vivo. *Dev Biol.* 2001;230:230–242.
48. Griffith TM, Chaytor AT, Edwards DH. The obligatory link: role of gap junctional communication in endothelium-dependent smooth muscle hyperpolarization. *Pharmacol Res.* 2004;49:551–564.
49. Saliez J, Bouzin C, Rath G, et al. Role of caveolar compartmentation in endothelium-derived hyperpolarizing factor-mediated relaxation: $Ca^{2+}$ signals and gap junction function are regulated by caveolin in endothelial cells. *Circulation* 2008;117:1065–1074.